

# Topological flat band, Dirac fermions and quantum spin Hall phase in 2D Archimedean lattices

F. Crasto de Lima,\* Gerson J. Ferreira, and R. H. Miwa  
*Instituto de Física, Universidade Federal de Uberlândia,*  
*C.P. 593, 38400-902, Uberlândia, MG, Brazil*  
 (Dated: August 15, 2019)

Materials with designed properties arises in a synergy between theoretical and experimental approaches. In this study we explore the set of Archimedean lattices forming a guidance to its electronic properties and topological phases. Within these lattices, rich electronic structure emerge forming type-I and II Dirac fermions, topological flat bands and high-degeneracy points with linear and flat dispersions. Employing a tight-binding model, with spin-orbit coupling, we characterize a quantum spin Hall (QSH) phase in all Archimedean lattices. Our discussion is validated within density functional theory calculations, where we show the characteristic bands of the studied lattices arising in 2D carbon allotropes.

## I. INTRODUCTION

Since the experimental discovery of graphene<sup>1</sup> two-dimensional (2D) materials have become the subject of numerous studies<sup>2,3</sup>. Correspondingly, the family of 2D materials have increased in recent years with the synthesis of new materials, e.g. transition metal-dichalcogenides<sup>4</sup>, borophene<sup>5</sup>, gallenene<sup>6</sup>, and many others<sup>7</sup>. In synergy with the experiments, high throughput calculations have bring into evidence new 2D phases<sup>8,9</sup>.

In these lower dimensional materials there is an emergence of phenomena prominent for applications. Particularly, the graphene Dirac fermions<sup>10</sup>, quantum spin, anomalous, valley and fractional Hall phases<sup>11–15</sup>, but also electronics based in the valley<sup>16</sup>, layer<sup>17</sup> and cone<sup>18</sup> degrees of freedom. On the other hand, monoatomically flat materials like graphene are still rare compared with the vast 2D materials class. Interesting properties arise in such class of materials, for instance, the perfectly flat structure of kagome and Lieb lattices presents a topological flat band<sup>19</sup> and fractional quantum Hall effect<sup>20</sup>. Moreover, high degeneracy points in the band structure allows exotic fermions to emerge<sup>21–24</sup>. Therefore, a focused research in new 2D lattices can uncover quasi-particles (e.g., of the Dirac, Weyl and Kane types) in condensed-matter physics.

Although all possible periodical arrangement of sites in a plane is inconceivable large, there exist classes of 2D crystals that remain with its electronic properties unexploited. For instance, classes of lattices generated by considering one site in every vertex of the  $k$ -uniform tiling of the plane<sup>25</sup>, where  $k$  is the number of nonequivalent vertexes. The most simple lattices are given by  $k = 1$ , i.e. only one nonequivalent vertex, namely uniform tiling, also known as Archimedean lattices, which are shown in Fig. 1. The notation taken to classify these lattice is to list the types of polygons forming each vertex and the times it appears, for instance  $(4, 8^2)$  indicates that each vertex is surrounded by one square and two octagons. Particularly, the well known graphene  $(6^3)$  and kagome

$(3, 6, 3, 6)$  lattices belong to the class of Archimedean lattices.

From a theoretical point of view Archimedean lattices have been explored showing magnetic frustration<sup>26</sup>, and possible formation in photonic crystals<sup>27</sup>, where its topological phases are still unexploited. The design of photonic crystals allow highly controllable formation of structures, increasing the possible exploration of the Archimedean lattices<sup>28</sup>. Additionally, beyond graphene and kagome lattices, there are other proposed and synthesized materials with Archimedean lattices, e.g. the graphenylene<sup>29</sup> with a  $(4, 6, 12)$  structure, and 2D allotropes of boron with  $(3^4, 6)$ <sup>30,31</sup> and  $(3^3, 4^2)$ <sup>32</sup> structures. Moreover, 2D metal-organic frameworks<sup>33–35</sup> have recently been gaining attention. In such systems a particular lattice structure can be designed by combining different metals and molecular ligands. Furthermore, a recent study has identified the distinct interparticle interactions needed to allow the self-assembly of the studied lattices<sup>36</sup>.

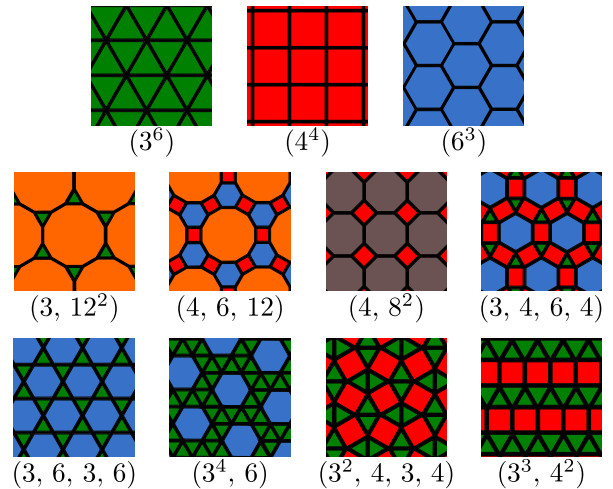


FIG. 1. All eleven Archimedean lattices or uniform tilings, in which all polygons are regular and each vertex is surrounded by the same sequence of polygons.

In this paper we explore the electronic properties arising due to the flat structure of the Archimedean lattices. We provide a detailed band structure analysis with respect to single orbital tight-binding models. Therefore, our results can be directly interpreted in different quasiparticle systems, e.g. photonic<sup>28</sup>, phononic<sup>37,38</sup>, magnonic<sup>39</sup>. Moreover, including the intrinsic spin-orbit coupling to the model, we explore the quantum spin Hall phases in electronic systems. Additionally, we validate our discussion presenting materials realizations of the Archimedean lattices.

## II. METHOD

To study the Archimedean lattices we consider a single orbital per site tight-binding (TB) Hamiltonian. Throughout the paper we will discuss first the systems without spin-orbit coupling (SOC), and subsequently in the presence of SOC<sup>15,40</sup>. As the proposed systems are mirror symmetric in the plane of the sites, the Rashba SOC has null contributions. Therefore, the Hamiltonian can be written as

$$H_{TB} = H_0 + H_{SO}, \quad (1)$$

where each term is given by

$$H_0 = \sum_i \varepsilon_i c_i^\dagger \sigma_0 c_i + \sum_{i,j} t_{ij} c_i^\dagger \sigma_0 c_j, \quad (2)$$

$$H_{SO} = i \sum_{i,j} \lambda_{ij} c_i^\dagger \boldsymbol{\sigma} \cdot (\mathbf{d}_{kj} \times \mathbf{d}_{ik}) c_j. \quad (3)$$

Here,  $c_i^\dagger = (c_{i\uparrow}^\dagger, c_{i\downarrow}^\dagger)$  and  $c_i = (c_{i\uparrow}, c_{i\downarrow})^T$  are the creation and annihilation operators for an electron on site  $i$  and spin  $\uparrow$  or  $\downarrow$ ;  $\boldsymbol{\sigma} = (\sigma_x, \sigma_y, \sigma_z)$  are the spin Pauli matrices,  $\mathbf{d}_{ij}$  is the vector connecting the  $i$ th and  $j$ th sites;  $\varepsilon_i$ ,  $t_{ij}$ ,  $\lambda_{ij}$  are the on-site energies and strength of hopping and spin-orbit terms. In order to parametrize the Hamiltonian we have considered the hopping and spin-orbit terms exponentially decaying with the inter-site distance

$$t_{ij} = -N t \exp\{-\alpha d_{ij}\}, \quad (4)$$

$$\lambda_{ij} = N \lambda \exp\{-\alpha d_{ij}\}. \quad (5)$$

All energies are normalized to the nearest-neighbor (NN) hopping,  $N = \exp\{\alpha d_{nn}\}$ , with  $d_{nn}$  the NN distance, and taking  $t = 1$  as the energy unit. Within this definition the parameter  $\alpha$  controls the contribution of the next nearest-neighbor (NNN) and, further neighbors, in relation to the NN. Therefore for  $\alpha \gg d_{nn}^{-1}$  only NN terms are relevant, while for small  $\alpha$  the NNN and further terms strength increases.

## III. RESULTS

We will focus on the Archimedean lattices formed by more than one type of polygon tiling, as the first three lattices of Fig. 1, namely  $(3^6)$ ,  $(4^4)$  and the graphene  $(6^3)$  lattices are well known and extensively studied<sup>10</sup>. For the remaining eight lattices we have planar three fold coordination sites  $[(3, 12^2), (4, 6, 12)$  and  $(4, 8^2)]$ , four fold  $[(3, 4, 6, 4)$  and  $(3, 6, 3, 6)]$  and five fold  $[(3^4, 6), (3^2, 4, 3, 4)$  and  $(3^3, 4^4)]$ . Interestingly, all Archimedean lattices are composed by only one Wyckoff position<sup>41</sup>. The hexagonal  $(3, 12^2)$ ,  $(4, 6, 12)$ ,  $(3, 4, 6, 4)$ ,  $(3, 6, 3, 6)$  lattices transform as the  $P6/mmm$  space group and are constructed by the Wyckoff point m, q, m and g respectively. The  $(3^4, 6)$  hexagonal lattice transform as  $P6/m$  space group and the k Wyckoff position. The square lattices  $(4, 8^2)$  and  $(3^2, 4, 3, 4)$  transform respectively as  $P4/mmm$  and  $P4/mbm$  space groups, with m and h Wyckoff positions. Lastly, the oblique  $(3^3, 4^2)$  lattice transform as  $Cmmm$  space group and with the j Wyckoff position.

As we will shown in the following sections, the Archimedean lattices present a rich electronic structure, ranging from flat bands to multiply degenerated Dirac cones.

### A. Archimedean band structure

In this section we discuss the Archimedean lattices band structure without SOC, which can be implemented in photonic crystals and direct related to other quasiparticle systems.

Recently, the appearance of flat bands in materials was given a lot of attention, for instance in photonics<sup>42</sup> due to its analogy with frustrated magnetism<sup>43</sup> and possible fractional quantum Hall phase<sup>44,45</sup>. Interestingly, in the Archimedean lattices there are various occurrences of partially flat or fully flat bands. For the well known kagome  $(3, 6, 3, 6)$  lattice<sup>46</sup>, a perfectly flat band (FB) occur only for NN hopping [FB in Fig. 2(e1)], while considering further neighbor hoppings it gains a small dispersion [Fig. 2(e2)], increasing with the NNN hopping strength. A similar case can be observed in the  $(3, 12^2)$  lattice, where two flat bands enclose dispersive graphene-like bands [FB in Fig. 2(a1)]. For this lattice the effect of NNN hopping change mostly the bandwidth without changing the flatness of the FB.

Besides the perfect flat bands appearing in the whole Brillouin Zone, partially flat (PF) bands are also present in the studied systems. For instance, in the  $(4, 6, 12)$  lattice we can see flat bands occurring in the  $\Gamma$ -M direction in the 4th and, due to chiral symmetry, 9th band [PF in Fig. 2(b1)], while considering NNN hopping [Fig. 2(b2)] such symmetry is broken with the PF bands becoming dispersive. A similar case occur at the  $(4, 8^2)$  and  $(3^4, 6)$  lattices, where in the former the 2nd (3rd) band is flat in the X-M ( $\Gamma$ -X) direction [PF in Fig. 2(c1)], while in the latter the 4th band is flat in the  $\Gamma$ -M direction [PF

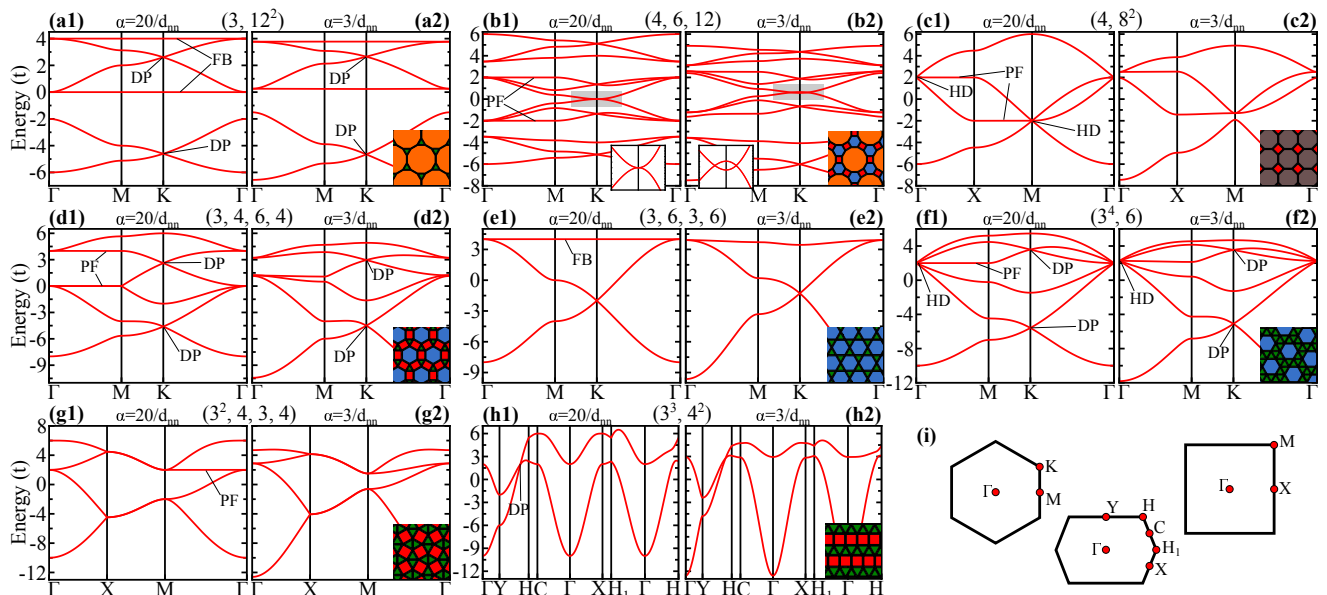


FIG. 2. Band structure for  $\alpha = 20.0/d_{nn}$  (a1)-(h1) and  $\alpha = 3.0/d_{nn}$  (a2)-(h2), without SOC ( $\lambda = 0$ ). We also show the 1st Brillouin Zones and the symmetry points (i) for the hexagonal, square and oblique lattices. Within the band plots we have labeled the Dirac points (DP), flat bands (FB), partially flat (PF) bands and high degeneracy (HD) points.

in Fig. 2(f1)]. In this two lattices, considering further neighbors hopping do not present significant effects in the flat bands. The absence of the NNN effect on the flat bands is different for the  $(3, 4, 6, 4)$  and  $(3^2, 4, 3, 4)$  lattices, where the flat bands in the  $\Gamma$ -M [PF in Fig. 2(d1)] and M- $\Gamma$  [PF in Fig. 2(g1)] direction become dispersive for NNN hopping [Fig. 2 (d2) and (g2)].

Another highly studied feature appearing in materials in general are the linear Dirac-like dispersions. Such energy spectrum is responsible for the high mobility in graphene, and many other phenomena<sup>10</sup>. In the class of Archimedean lattices, linear dispersive Dirac points (DP) are presented in different manners in all structures. For instance we can see two evident Dirac cone dispersions in the  $K$ -point of the lattices  $(3, 12^2)$  [DP Fig. 2(a)],  $(3, 4, 6, 4)$  [DP Fig. 2(d)] and  $(3^4, 6)$  [DP Fig. 2(f)], which are still present even considering second neighbors hoppings. In the  $(4, 6, 12)$  lattice a symmetry analysis show that the  $K$ -point allow four doubly degenerated and two unidimensional irreducible representations. Looking at the NN band structure [Fig. 2(b1)] we find 5 points with double degenerated bands, which means that one of them is an accidental degeneracy. All except one (shaded region) of this double degenerated bands have linear cone-like dispersion. By taking NNN hopping into consideration we can see that the non-linear crossing opens a gap at the  $K$ -point [Fig. 2(b2) inset]. On the other hand, this two bands are still degenerated close to the  $K$ -point, forming a Dirac nodal line enclosing such point.

Different from the symmetric type-I Dirac cone dispersion appearing in the kagome  $(3, 6, 3, 6)$  lattice [Fig. 2(e1)-(e2)], in the  $(3^3, 4^2)$  lattice we see a tilted linear crossing [DP in Fig. 2(h1)-(h2)], i.e. type-II

Dirac quasiparticle. Such feature, appearing also in borophene<sup>47</sup>, and transition-metal dichalcogenides<sup>48,49</sup>, have a non-trivial Berry phase<sup>50</sup>. Lastly, in the  $(3^2, 4, 3, 4)$  lattice a linear, but not conical, dispersion can be observed along wave vectors crossing the X-M direction. Such feature form a nodal line in the border of the Brillouin Zone, with the linear dispersion for vectors crossing this line.

High degeneracy (HD) points in the band structure allows exotic fermions to emerge<sup>21,22</sup>. For instance, a hybrid state between a pseudospin 1 and pseudospin 1/2, also know as Kane fermion, have been observed in an 2D MOF<sup>22</sup>. A signature of such fermion is a flat band forming a three-fold degeneracy with a Dirac cone. Interesting we find in the  $(4, 8^2)$  lattice two points with a pseudospin-1 Dirac dispersion, at the  $\Gamma$  and  $M$  [HD Fig. 2(c1)]. On the other hand taking the NNN hopping into consideration its degeneracy is lowered [Fig. 2(c2)]. A different scenario appears in the  $(3^4, 6)$  lattice, where at the  $\Gamma$  point we find two Dirac cones, with different velocities, degenerated with a flat band, forming a pseudospin-2 Dirac dispersion [HD in Fig. 2(f1)-(f2)]. In this case the degeneracy is still present even considering NNN hopping.

In the following section we will discuss the effect of SOC to the Archimedean lattices band structures, and characterize the emergent quantum spin Hall phases.

## B. QSH phase induced by SOC

In order to characterize the possible QSH phases in the Archimedean lattices, we take the SOC term into account. Usually, the opening of an energy gap, in previous

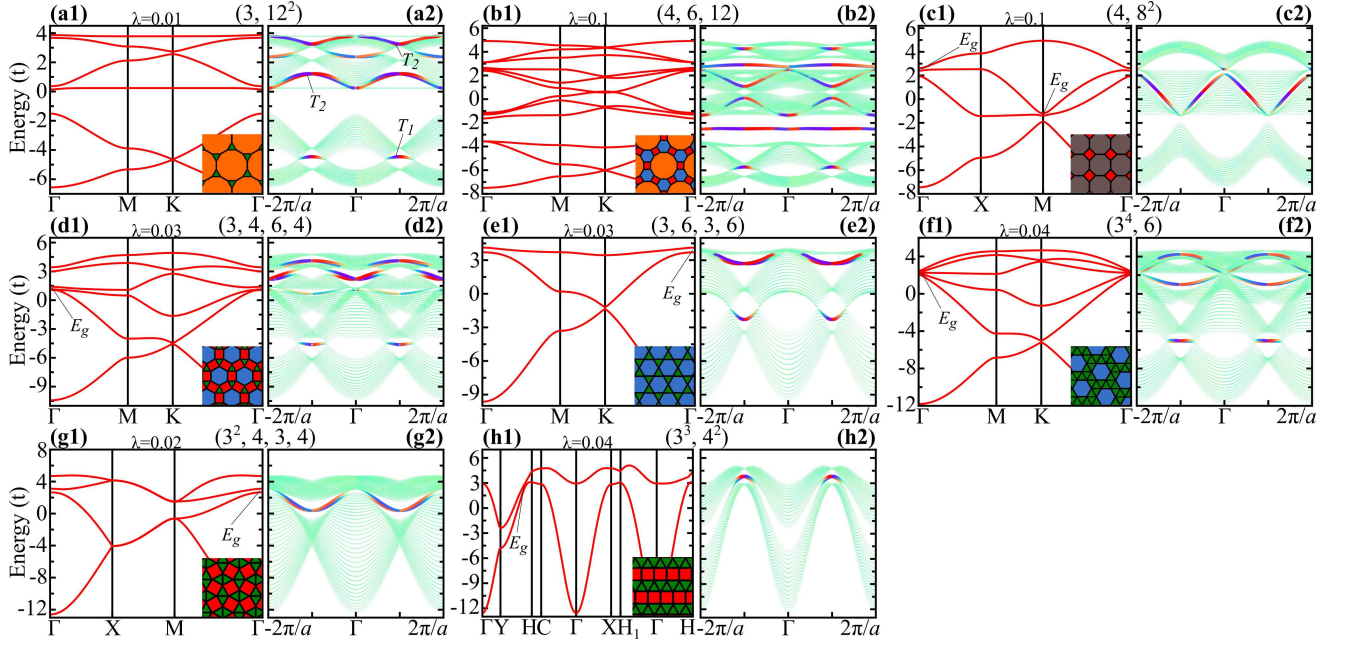


FIG. 3. Band structure with SOC and NNN hoppings ( $\alpha = 3.0/d_{nn}$ ) (a1)-(h1). Nanoribbons band structure with projected contribution of the edge sites (a2)-(h2), the size of each line is proportional to the edge contribution and the color is the  $S_z$  spin projection. Within the plots,  $E_g$  labels the energy gaps, while  $T_1$  and  $T_2$  the backscattering protected edge states.

degenerated bands, due to the atomic SOC, is a signature of QSH phase<sup>40</sup>.

By considering the SOC term, within the NNN hopping bands of Fig. 2(a2)-(h2) we see the gap opening on some of the degenerated points, as show in Fig. 3. For instance, for all hexagonal lattices, at the Dirac points we see a gap opening. Additionally, the degeneracy points of a flat band and the Dirac cones at the  $\Gamma$  point also presents a gap opening, e.g. the gap at  $E = 4.0t$  on the  $(3, 6, 3, 6)$  lattice [ $E_g$  in Fig. 3(e1)]. In particular, the triple degeneracy of  $(3, 4, 6, 4)$   $\Gamma$  point around  $E = 1.0t$  also breaks into three non-degenerated points [ $E_g$  in Fig. 3(d1)]. The same occur to the quintuple degeneracy at  $(3^4, 6)$   $\Gamma$  point at  $E = 2.5t$  [ $E_g$  in Fig. 3(f1)]. For the square lattice  $(4, 8^2)$  the degeneracy of  $\Gamma$  and  $M$  points are broken, as in the non-symmorphic lattice  $(3^3, 4, 3, 4)$   $\Gamma$  point [ $E_g$  in Fig. 3(c1) and (g1)]. In contrast, the degeneracy at  $X$ - $M$  direction arising from the non-symmorphic symmetry is preserved. Lastly the accidental degeneracy of the tilted Dirac cone in the oblique  $(3^3, 4^2)$  lattice also become gaped with the inclusion of the SOC.

To characterize the existence of the QSH phases, we have tracked the Wannier charge centers evolution<sup>51,52</sup> to determine the  $Z_2$  topological invariant. A summary of the  $Z_2$  index as a function of the Kramers pair bands occupation is shown in Fig. 4. Interestingly all studied lattices presents in some particular occupation a QSH phase. For instance, as stated, in all Dirac cones the SOC lead to a QSH edge state. To highlight a few cases, in the  $(3, 12^2)$  lattice [black circles in Fig. 4] a  $Z_2 = 1$  phase

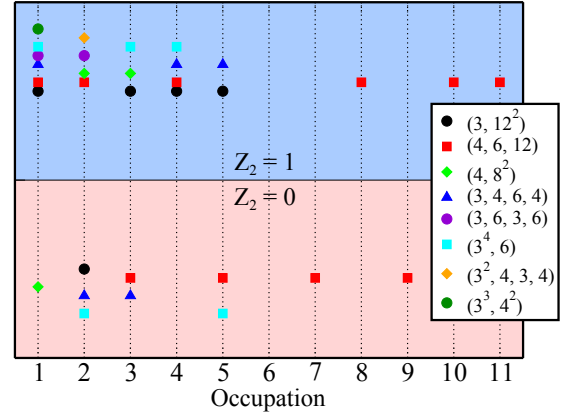


FIG. 4. Calculated  $Z_2$  invariant for different number of occupied Kramers pairs bands. The occupation number indicates the number of occupied Kramer pairs bands starting in the lowest energy.

is observed for the occupation of the first Kramer pair of bands, i.e. the Fermi level being in the lower Dirac point of Fig. 3(a1). Indeed, computing the edge states band projection we find spin-textured bands within the same energy window,  $T_1$  in Fig. 3(a2). Beside the Dirac points, the degeneracy point between a flat and dispersive bands also lead to the QSH phase, e.g. the 4th and 6th occupation of  $(3, 12^2)$  lattice in Fig. 3(a1) has  $Z_2 = 1$  [Fig. 4]. In turn, it leads to the backscattering protected edge states, shown by  $T_2$  in Fig. 3(a2). A particular case occur in the hexagonal  $(4, 6, 12)$ , where the SOC do not



open the accidental degeneracy Dirac node between 6th and 7th band [Fig. 3(b1)], which in turn do not have a defined  $Z_2$  invariant. The same occur also for the non-symmorphic symmetry protected degeneracy between 1st and 2nd bands of  $(3^2, 4, 3, 4)$  [Fig. 3(g1)].

The application of the results above rely on the synthesis of materials in Archimedean lattices structures. In the next section we discuss the material realization of the Archimedean lattices, while as a proof of principle we have characterized the existence of its characteristic band dispersions arising in carbon allotropes.

### C. Materials realization of Archimedean lattices

It is interesting to point out that materials with Archimedean lattices are already proven theoretically and experimentally to exist. First, graphene<sup>1</sup>, the most studied 2D material, is the immediate example of the  $(6^3)$  Archimedean lattice. Experimentally, self-assembly of molecules in surfaces lead to a variety of possible structures, where structures equivalent to the  $(3, 4, 6, 4)$ <sup>53</sup>,  $(3^4, 6)$ <sup>54</sup> and  $(3^2, 4, 3, 4)$ <sup>55</sup> have been observed. By using *first-principles* calculations, it was predicted materials with the Archimedean lattices, e.g. graphenylene, an allotrope of carbon, presents the  $(4, 6, 12)$  lattice<sup>29</sup>. Also, a 2D boron sheet form the  $(3^4, 6)$  structure<sup>31</sup>. Bellow, as a proof of principle, we present three other Archimedean lattices and show the presence of its characteristic electronic dispersion.

Here, by using *first-principles* calculations, based in the density functional theory (DFT), we focus in the monoatomic layers of carbon allotropes. Within the VASP<sup>56</sup> code we relax the atomic positions and lattice vectors, until the force in each atom was less than 1 meV/Å. We have considered the PBE<sup>57</sup> functional to describe exchange and correlation term, with the projector augmented-wave<sup>58</sup> method for the electron-ion interaction. The wave functions were expanded in a plane-wave basis with cutoff energy of 500 eV. For BZ integration, a  $11 \times 11 \times 1$  k-mesh was considered. For the calculations of the force constants we considered a  $3 \times 3$  supercell with energy convergence criteria of at least  $10^{-8}$  eV.

TABLE I. Lattice parameter  $a$  (Å), average nearest neighbor distance  $\langle d_{cc} \rangle$  (Å), and its root mean-square deviation  $\langle \delta d \rangle = \sqrt{\langle d_{cc}^2 \rangle - \langle d_{cc} \rangle^2}$  (Å). Formation energy  $E_f = E_{\text{Arc}} - E_G$  (eV/atom), where  $E_{\text{Arc}}$  is the total energy per atom of the Archimedean lattice and  $E_G$  is the total energy per atom of graphene.

| Lattice      | state | $a$   | $\langle d_{cc} \rangle$ | $\langle \delta d_{cc} \rangle$ | $E_f$ |
|--------------|-------|-------|--------------------------|---------------------------------|-------|
| $(3, 12^2)$  | flat  | 5.143 | 1.401                    | 0.033                           | 0.969 |
| $(4, 6, 12)$ | flat  | 6.768 | 1.439                    | 0.051                           | 0.633 |
| $(4, 8^2)$   | flat  | 3.446 | 1.435                    | 0.044                           | 0.513 |

In two-dimensions, carbon atoms usually form the planar 3-fold coordinated  $sp^2$  hybridization. Naturally,

satisfying this geometry, the carbon atoms could form the  $(3, 12^2)$ ,  $(4, 6, 12)$  and  $(4, 8^2)$  lattices. In fact, as shown in Tab. I, this carbon lattices present formation energy close to the already synthesized graphyne phase ( $\sim 0.7$  eV/atom)<sup>59,60</sup>. To find the stability of the Archimedean carbon lattices we have calculated the phonon spectra, as shown in Fig. 5(a1)-(c1), where no negative frequencies were find, in agreement with previous study<sup>61</sup>. Furthermore, in the ground state structure we find mean carbon-carbon distance ( $\langle d_{cc} \rangle$ ) with a deviation of only 1% in relation to the graphene lattice ( $d_{cc} = 1.42$  Å), as shown in Table I. However, a fluctuation in  $d_{cc}$  is observed for nonequivalent bond directions, which we can see from the charge density map in the inset of Fig. 5(a1)-(c1), with dark red regions indicating greater charge density, correlated with smaller  $d_{cc}$ . Nevertheless, this bond distance variation do not modify the space group in relation to the perfect Archimedean lattice.

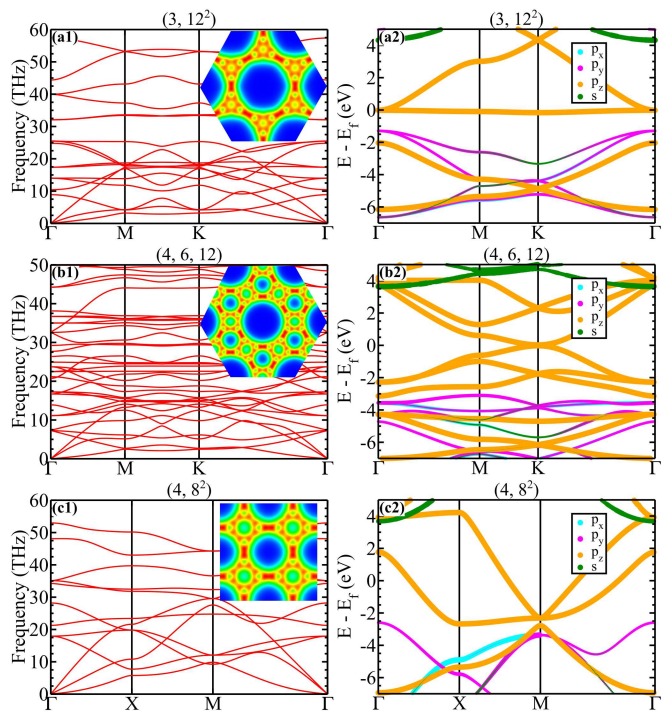


FIG. 5. Phonon dispersion (a1)-(c1) and orbital projected band structure (a2)-(c2) for the three folded carbon lattices (a)  $(3, 12^2)$ , (b)  $(4, 6, 12)$  and (c)  $(4, 8^2)$ . The inset in the left side plot shown the charge density map in the plane with red (blue) indicate high (low) density regions.

The planar geometry of this systems will lead to a decoupling of the carbon  $p$  orbitals, in the even ( $p_x/p_y$ ) and odd ( $p_z$ ) in-plane mirror symmetries. Furthermore, the  $p_z$  orbitals have azimuthal symmetry, therefore the interaction with neighbouring  $p_z$  will be only distance dependent. The proposed TB hamiltonian of the second section has exactly this picture, in turn it will capture the bands formed by the carbon  $p_z$  orbitals. First for the  $(3, 12^2)$  lattice, note that the  $p_z$  orbitals, orange cir-

cles in Fig. 5(a2), form the low energy Dirac crossing and structure of flat bands enclosing Dirac dispersion, found in Fig. 2(a1), with the flat band resonant in the Fermi energy. Such occupation configuration is exactly one that has a  $Z_2 = 1$  phase with the inclusion of SOC. For the (4, 6, 12) lattice, Fig. 5(b2), the Fermi level is exactly in the accidental highlighted crossing shown in the inset of Fig. 2(b1). However, due to the higher bond distance variation ( $(\delta d_{cc})$ ), this accidental degeneracy is lifted by a energy gap of 50 meV. Nonetheless, the Dirac crossings are still preserved in 2.3 eV ( $-1.8$  eV) above (below) the Fermi level. Lastly, in the most stable (4, 8<sup>2</sup>) lattice, the  $p_z$  orbitals show a breaking of the three-fold degeneracy in the  $M$ -point, Fig. 5(c2). Such feature indicates the relevance of NNN neighbours hopping, compare for instance with Fig. 2(c1)-(c2). Furthermore, external perturbations allow the control of these Archimedean bands. For instance, an isotropic strain field will change the atoms distance allowing a control of the NN and further neighbour hopping percentage, while proximity effects can induce SOC leading to the QSH effect<sup>62</sup>

#### IV. SUMMARY

The Archimedean lattices presents rich electronic structure. For instance, we find type-I and II Dirac crossings and flat bands. Additionally, high degeneracy points, associated with pseudospin-1 and -2 Dirac quasiparticles have been found. The inclusion of spin-orbit couplings lead to topological energy gaps, where we construct a map to the occupation with backscattering protected edge states. Finally, our lattice tight binding model is corroborated by showing, within *first-principles* calculations, the existence of the characteristic Archimedean bands in stable 2D carbon allotropes. These results work as a guide for exploration of designed 2D lattices.

#### ACKNOWLEDGMENTS

The authors acknowledge financial support from the Brazilian agencies CNPq, and FAPEMIG, and the CENAPAD-SP and Laboratório Nacional de Computação Científica (LNCC-SCAFMat) for the computer resources.

\* felipe.lima@ufu.br

- <sup>1</sup> K. S. Novoselov, A. K. Geim, S. V. Morozov, D. Jiang, Y. Zhang, S. V. Dubonos, I. V. Grigorieva, and A. A. Firsov, “Electric Field Effect in Atomically Thin Carbon Films,” *Science* **306**, 666–669 (2004).
- <sup>2</sup> H. Cheun Lee, Wei-Wen Liu, Siang-Piao Chai, Abdul Rahman Mohamed, Azizan Aziz, Cheng-Seong Khe, N.M. S. Hidayah, and U. Hashim, “Review of the synthesis, transfer, characterization and growth mechanisms of single and multilayer graphene,” *RSC Adv.* **7**, 15644–15693 (2017).
- <sup>3</sup> Andrew J. Mannix, Brian Kiraly, Mark C. Hersam, and Nathan P. Guisinger, “Synthesis and chemistry of elemental 2d materials,” *Nature Reviews Chemistry* **1**, 0014 (2017), review Article.
- <sup>4</sup> Sajedeh Manzeli, Dmitry Ovchinnikov, Diego Pasquier, Oleg V. Yazyev, and Andras Kis, “2D transition metal dichalcogenides,” *Nature Reviews Materials* **2**, 17033 (2017).
- <sup>5</sup> Zhuhua Zhang, Evgeni S. Penev, and Boris I. Yakobson, “Two-dimensional boron: structures, properties and applications,” *Chem. Soc. Rev.* **46**, 6746–6763 (2017).
- <sup>6</sup> Vidya Kochat, Atanu Samanta, Yuan Zhang, Sanjit Bhowmick, Praveena Manimunda, Syed Asif S. Asif, Anthony S. Stender, Robert Vajtai, Abhishek K. Singh, Chandra S. Tiwary, and Pulickel M. Ajayan, “Atomically thin gallium layers from solid-melt exfoliation,” *Science Advances* **4** (2018), 10.1126/sciadv.1701373.
- <sup>7</sup> Dechao Geng and Hui Ying Yang, “Recent Advances in Growth of Novel 2D Materials: Beyond Graphene and Transition Metal Dichalcogenides,” *Advanced Materials* **30**, 1800865 (2018).
- <sup>8</sup> Nicolas Mounet, Marco Gibertini, Philippe Schwaller, Davide Campi, Andrius Merkys, Antimo Marrazzo, Thibault Sohier, Ivano Eligio Castelli, Andrea Cepellotti, Giovanni Pizzi, and Nicola Marzari, “Two-dimensional materials from high-throughput computational exfoliation of experimentally known compounds,” *Nature Nanotechnology* **13**, 246–252 (2018).
- <sup>9</sup> Sten Haastrup, Mikkel Strange, Mohnish Pandey, Thorsten Deilmann, Per S Schmidt, Nicki F Hinsche, Morten N Gjerding, Daniele Torelli, Peter M Larsen, Anders C Riis-Jensen, Jakob Gath, Karsten W Jacobsen, Jens Jørgen Mortensen, Thomas Olsen, and Kristian S Thygesen, “The Computational 2D Materials Database: high-throughput modeling and discovery of atomically thin crystals,” *2D Materials* **5**, 042002 (2018).
- <sup>10</sup> A. H. Castro Neto, F. Guinea, N. M. R. Peres, K. S. Novoselov, and A. K. Geim, “The electronic properties of graphene,” *Rev. Mod. Phys.* **81**, 109–162 (2009).
- <sup>11</sup> C. L. Kane and E. J. Mele, “Quantum Spin Hall Effect in Graphene,” *Phys. Rev. Lett.* **95**, 226801 (2005).
- <sup>12</sup> K. Hatsuda, H. Mine, T. Nakamura, J. Li, R. Wu, S. Katsumoto, and J. Haruyama, “Evidence for a quantum spin Hall phase in graphene decorated with Bi<sub>2</sub>Te<sub>3</sub> nanoparticles,” *Science Advances* **4** (2018), 10.1126/sciadv.aau6915.
- <sup>13</sup> Katsuyosih Komatsu, Yoshifumi Morita, Eiichiro Watanabe, Daiju Tsuya, Kenji Watanabe, Takashi Taniguchi, and Satoshi Moriyama, “Observation of the quantum valley Hall state in ballistic graphene superlattices,” *Science Advances* **4** (2018), 10.1126/sciadv.aaq0194.
- <sup>14</sup> P. M. Ostrovsky, I. V. Gornyi, and A. D. Mirlin, “Theory of anomalous quantum Hall effects in graphene,” *Phys. Rev. B* **77**, 195430 (2008).
- <sup>15</sup> Evelyn Tang, Jia-Wei Mei, and Xiao-Gang Wen, “High-Temperature Fractional Quantum Hall States,” *Phys. Rev. Lett.* **106**, 236802 (2011).

- <sup>16</sup> Yee Sin Ang, Shengyuan A. Yang, C. Zhang, Zhongshui Ma, and L. K. Ang, "Valleytronics in merging Dirac cones: All-electric-controlled valley filter, valve, and universal reversible logic gate," *Phys. Rev. B* **96**, 245410 (2017).
- <sup>17</sup> F. Crasto de Lima, G. J. Ferreira, and R. H. Miwa, "Layertronic control of topological states in multilayer metal-organic frameworks," *The Journal of Chemical Physics* **150**, 234701 (2019).
- <sup>18</sup> Menghao Wu, Zhijun Wang, Junwei Liu, Wenbin Li, Huahua Fu, Lei Sun, Xin Liu, Minghu Pan, Hongming Weng, Mircea Dincă, Liang Fu, and Ju Li, "Conetronics in 2D metal-organic frameworks: double/half Dirac cones and quantum anomalous Hall effect," *2D Materials* **4**, 015015 (2016).
- <sup>19</sup> Wei Jiang, Meng Kang, Huaqing Huang, Hongxing Xu, Tony Low, and Feng Liu, "Topological band evolution between Lieb and kagome lattices," *Phys. Rev. B* **99**, 125131 (2019).
- <sup>20</sup> Shou-Shu Gong, Wei Zhu, and D. N. Sheng, "Emergent Chiral Spin Liquid: Fractional Quantum Hall Effect in a Kagome Heisenberg Model," *Scientific Reports* **4**, 6317 (2014).
- <sup>21</sup> Barry Bradlyn, Jennifer Cano, Zhijun Wang, M. G. Vergniory, C. Felser, R. J. Cava, and B. Andrei Bernevig, "Beyond Dirac and Weyl fermions: Unconventional quasiparticles in conventional crystals," *Science* **353** (2016), 10.1126/science.aaf5037.
- <sup>22</sup> Aizhu Wang, Xinrui Zhao, Mingwen Zhao, Xiaoming Zhang, Yuanping Feng, and Feng Liu, "Kane Fermion in a Two-Dimensional  $\pi$ -Conjugated Bis(iminothiolato)nickel Monolayer," *The Journal of Physical Chemistry Letters* **9**, 614–619 (2018).
- <sup>23</sup> Minwoo Park, Youngkuk Kim, and Hoonkyung Lee, "Design of 2D massless Dirac fermion systems and quantum spin Hall insulators based on sp-sp<sup>2</sup> carbon sheets," *npj Computational Materials* **4**, 54 (2018).
- <sup>24</sup> T. Tzen Ong and Naoto Nagaosa, "Spin Transport and Accumulation in a 2D Weyl Fermion System," *Phys. Rev. Lett.* **121**, 066603 (2018).
- <sup>25</sup> Branko Grunbaum and Geoffrey C. Shephard, "Tilings by Regular Polygons," *Mathematics Magazine* **50**, 227–247 (1977).
- <sup>26</sup> Unjong Yu, "Ising antiferromagnet on the Archimedean lattices," *Phys. Rev. E* **91**, 062121 (2015).
- <sup>27</sup> Kazunari Ueda, Tomonari Dotera, and Tohru Gemma, "Photonic band structure calculations of two-dimensional Archimedean tiling patterns," *Phys. Rev. B* **75**, 195122 (2007).
- <sup>28</sup> Alexander B. Khanikaev and Gennady Shvets, "Two-dimensional topological photonics," *Nature Photonics* **11**, 763–773 (2017).
- <sup>29</sup> Qi Song, Bing Wang, Ke Deng, Xinliang Feng, Manfred Wagner, Julian D. Gale, Klaus Mullen, and Linjie Zhi, "Graphenylene, a unique two-dimensional carbon network with nondelocalized cyclohexatriene units," *J. Mater. Chem. C* **1**, 38–41 (2013).
- <sup>30</sup> Hui Tang and Sohrab Ismail-Beigi, "First-principles study of boron sheets and nanotubes," *Phys. Rev. B* **82**, 115412 (2010).
- <sup>31</sup> Wen-cai Yi, Wei Liu, Jorge Botana, Lei Zhao, Zhen Liu, Jing-yao Liu, and Mao-sheng Miao, "Honeycomb Boron Allotropes with Dirac Cones: A True Analogue to Graphene," *The Journal of Physical Chemistry Letters* **8**, 2647–2653 (2017).
- <sup>32</sup> Kah Chun Lau and Ravindra Pandey, "Stability and Electronic Properties of Atomistically-Engineered 2D Boron Sheets," *The Journal of Physical Chemistry C* **111**, 2906–2912 (2007).
- <sup>33</sup> John W. Colson and William R. Dichtel, "Rationally synthesized two-dimensional polymers," *Nat. Chem.* **5**, 453 (2013).
- <sup>34</sup> D. Rodriguez-San-Miguel, P. Amo-Ochoa, and F. Zamora, "MasterChem: cooking 2D-polymers," *Chem. Commun.* **52**, 4113–4127 (2016).
- <sup>35</sup> Norbert Stock and Shyam Biswas, "Synthesis of Metal-Organic Frameworks (MOFs): Routes to Various MOF Topologies, Morphologies, and Composites," *Chemical Reviews* **112**, 933–969 (2012).
- <sup>36</sup> Stephen Whitelam, "Minimal Positive Design for Self-Assembly of the Archimedean Tilings," *Phys. Rev. Lett.* **117**, 228003 (2016).
- <sup>37</sup> Bai-Zhan Xia, Ting-Ting Liu, Guo-Liang Huang, Hong-Qing Dai, Jun-Rui Jiao, Xian-Guo Zang, De-Jie Yu, Sheng-Jie Zheng, and Jian Liu, "Topological phononic insulator with robust pseudospin-dependent transport," *Phys. Rev. B* **96**, 094106 (2017).
- <sup>38</sup> Ziqi Yu, Zongqing Ren, and Jaeho Lee, "Phononic topological insulators based on six-petal holey silicon structures," *Scientific Reports* **9**, 1805 (2019).
- <sup>39</sup> Ryuichi Shindou, Ryo Matsumoto, Shuichi Murakami, and Jun-ichiro Ohe, "Topological chiral magnonic edge mode in a magnonic crystal," *Phys. Rev. B* **87**, 174427 (2013).
- <sup>40</sup> C. L. Kane and E. J. Mele, "Quantum Spin Hall Effect in Graphene," *Phys. Rev. Lett.* **95**, 226801 (2005).
- <sup>41</sup> U. Müller, "International Tables for Crystallography Volume A1: Symmetry relations between space groups," (2004), 10.1107/97809553602060000548.
- <sup>42</sup> Daniel Leykam and Sergej Flach, "Perspective: Photonic flatbands," *APL Photonics* **3**, 070901 (2018).
- <sup>43</sup> Zhiyong Lin, Jin-Ho Choi, Qiang Zhang, Wei Qin, Seho Yi, Pengdong Wang, Lin Li, Yifan Wang, Hui Zhang, Zhe Sun, Laiming Wei, Shengbai Zhang, Tengfei Guo, Qingyou Lu, Jun-Hyung Cho, Changgan Zeng, and Zhenyu Zhang, "Flatbands and Emergent Ferromagnetic Ordering in Fe<sub>3</sub>Sn<sub>2</sub> Kagome Lattices," *Phys. Rev. Lett.* **121**, 096401 (2018).
- <sup>44</sup> D. N. Sheng, Zheng-Cheng Gu, Kai Sun, and L. Sheng, "Fractional quantum Hall effect in the absence of Landau levels," *Nature Communications* **2**, 389 (2011).
- <sup>45</sup> Yi-Fei Wang, Hong Yao, Chang-De Gong, and D. N. Sheng, "Fractional quantum Hall effect in topological flat bands with Chern number two," *Phys. Rev. B* **86**, 201101 (2012).
- <sup>46</sup> C Barreteau, F Ducastelle, and T Mallah, "A bird's eye view on the flat and conic band world of the honeycomb and Kagome lattices: towards an understanding of 2D metal-organic frameworks electronic structure," *Journal of Physics: Condensed Matter* **29**, 465302 (2017).
- <sup>47</sup> Ganesh C. Paul, SK Firoz Islam, and Arijit Saha, "Fingerprints of tilted Dirac cones on the RKKY exchange interaction in 8-Pmmn borophene," *Phys. Rev. B* **99**, 155418 (2019).
- <sup>48</sup> Han-Jin Noh, Jinwon Jeong, En-Jin Cho, Kyoo Kim, B. I. Min, and Byeong-Gyu Park, "Experimental Realization of Type-II Dirac Fermions in a PdTe<sub>2</sub> Superconductor," *Phys. Rev. Lett.* **119**, 016401 (2017).
- <sup>49</sup> Huaqing Huang, Shuyun Zhou, and Wenhui Duan, "Type-II Dirac fermions in the PtSe<sub>2</sub> class of transition metal

- dichalcogenides,” *Phys. Rev. B* **94**, 121117 (2016).
- <sup>50</sup> Chunqiang Xu, Bin Li, Wenhe Jiao, Wei Zhou, Bin Qian, Raman Sankar, Nikolai D. Zhigadlo, Yanpeng Qi, Dong Qian, Fang-Cheng Chou, and Xiaofeng Xu, “Topological Type-II Dirac Fermions Approaching the Fermi Level in a Transition Metal Dichalcogenide NiTe<sub>2</sub>,” *Chemistry of Materials* **30**, 4823–4830 (2018).
- <sup>51</sup> Rui Yu, Xiao Liang Qi, Andrei Bernevig, Zhong Fang, and Xi Dai, “Equivalent expression of  $\mathbb{Z}_2$  topological invariant for band insulators using the non-Abelian Berry connection,” *Phys. Rev. B* **84**, 075119 (2011).
- <sup>52</sup> Alexey A. Soluyanov and David Vanderbilt, “Computing topological invariants without inversion symmetry,” *Phys. Rev. B* **83**, 235401 (2011).
- <sup>53</sup> Guoqing Lyu, Ran Zhang, Xin Zhang, Pei Nian Liu, and Nian Lin, “On-surface assembly of low-dimensional Pb-coordinated metalorganic structures,” *J. Mater. Chem. C* **3**, 3252–3257 (2015).
- <sup>54</sup> Linghao Yan, Guowen Kuang, Qiushi Zhang, Xuesong Shang, Pei Nian Liu, and Nian Lin, “Self-assembly of a binodal metalorganic framework exhibiting a demi-regular lattice,” *Faraday Discuss.* **204**, 111–121 (2017).
- <sup>55</sup> José I. Urgel, David Eciija, Willi Auwrtter, Anthoula C. Papageorgiou, Ari P. Seitsonen, Saranyan Vijayaraghavan, Sushobhan Joshi, Sybille Fischer, Joachim Reichert, and Johannes V. Barth, “Five-Vertex Lanthanide Coordination on Surfaces: A Route to Sophisticated Nanoarchitectures and Tessellations,” *The Journal of Physical Chemistry C* **118**, 12908–12915 (2014).
- <sup>56</sup> G. Kresse and J. Furthmüller, “Efficiency of ab-initio total energy calculations for metals and semiconductors using a plane-wave basis set,” *Comput. Mater. Sci.* **6**, 15 (1996).
- <sup>57</sup> John P. Perdew, Kieron Burke, and Matthias Ernzerhof, “Generalized Gradient Approximation Made Simple,” *Phys. Rev. Lett.* **77**, 3865–3868 (1996).
- <sup>58</sup> P. E. Blöchl, “Projector augmented-wave method,” *Phys. Rev. B* **50**, 17953–17979 (1994).
- <sup>59</sup> Guoxing Li, Yuliang Li, Huibiao Liu, Yanbing Guo, Yongjun Li, and Daoben Zhu, “Architecture of graphdiyne nanoscale films,” *Chem. Commun.* **46**, 3256–3258 (2010).
- <sup>60</sup> Mingwen Zhao, Wenzheng Dong, and Aizhu Wang, “Two-dimensional carbon topological insulators superior to graphene,” *Scientific Reports* **3**, 3532 (2013).
- <sup>61</sup> Xin-Quan Wang, Han-Dong Li, and Jian-Tao Wang, “Structural stabilities and electronic properties of planar C<sub>4</sub> carbon sheet and nanoribbons,” *Phys. Chem. Chem. Phys.* **14**, 11107–11111 (2012).
- <sup>62</sup> A. Avsar, J. Y. Tan, T. Taychatanapat, J. Balakrishnan, G. K. W. Koon, Y. Yeo, J. Lahiri, A. Carvalho, A. S. Rodin, E. C. T. O’Farrell, G. Eda, A. H. Castro Neto, and B. Özyilmaz, “Spin-orbit proximity effect in graphene,” *Nature Communications* **5**, 4875 (2014).